Raman measurements of phase transitions in dense solid hydrogen and deuterium to 325 GPa

Chang-sheng Zha[a], R. E. Cohen[a,b], Ho-kwang Mao[a,c], and Russell J. Hemley[a,1]

[a]Geophysical Laboratory, Carnegie Institution of Washington, Washington, DC 20015; [b]Department of Earth Sciences, University College London, London, United Kingdom; and [c]Center for High Pressure Science and Technology Advanced Research, Shanghai 201203, People's Republic of China

Contributed by Russell J. Hemley, February 18, 2014 (sent for review August 18, 2013)

Raman spectroscopy of dense hydrogen and deuterium performed to 325 GPa at 300 K reveals previously unidentified transitions. Detailed analysis of the spectra from multiple experimental runs, together with comparison with previous infrared and Raman measurements, provides information on structural modifications of hydrogen as a function of density through the I–III–IV transition sequence, beginning near 200 GPa at 300 K. The data suggest that the transition sequence at these temperatures proceeds by formation of disordered stacking of molecular and distorted layers. Weaker spectral changes are observed at 250, 285, and 300 GPa, that are characterized by discontinuities in pressure shifts of Raman frequencies, and changes in intensities and linewidths. The results indicate changes in structure and bonding, molecular orientational order, and electronic structure of dense hydrogen at these conditions. The data suggest the existence of new phases, either variations of phase IV, or altogether new structures.

diamond anvil cells | vibrational spectroscopy | molecular solids | high pressure

As element one, hydrogen has the simplest atomic structure, but its phase diagram is among the most poorly understood. Studying its physical properties under extreme pressure–temperature conditions has been an important subject in condensed matter physics during the past few decades (1, 2). Important advances have been made in studying the material experimentally and theoretically up to multimegabar (e.g., 300 GPa) pressures. Nevertheless, experiments are challenging because of difficulties in crystal structure determination and technical limitations in reaching a highly compressed state. Hydrogen has the smallest electron-scattering cross-section among all elements, resulting in extremely weak X-ray diffraction intensity for structure determination. Furthermore, the small sample volume at ultrahigh pressures provides an additional challenge for measurements of various other properties. In addition, hydrogen embrittlement causes failure in pressure confinement. Theoretically, the problem is particularly challenging because of the quantum dynamics of the nuclei (2).

Three high-pressure phases of solid hydrogen and deuterium exist to 200 GPa at or below room temperature. X-ray and neutron diffraction identified phase I as having a hexagonal close-packed structure; vibrational spectroscopy established that the structure is molecular, consists of quantum rotors, and has a wide pressure-temperature (*P-T*) range of stability. Phases II and III were identified by Raman and infrared absorption measurements, which currently are the most sensitive means for identifying phase transitions of these materials at multimegabar pressures. Recent advances in diamond anvil cell techniques have extended measurements of hydrogen to pressures above 300 GPa and temperatures above 300 K (3–9). Initial studies reported evidence for an electrically conducting state at 220 GPa at 296 K (3) and significant changes in optical and Raman spectra. The conductivity was reported to increase abruptly above 260 GPa and the Raman spectrum to disappear at ∼270 GPa, leading to the conclusion that a fully metallic state had been reached. A subsequent study to 315 GPa, also at room temperature, revealed similar Raman spectroscopic features (4), which were used to provide evidence for a transition to a new phase (phase IV). The observation of two vibrons with significant frequency difference has been explained as the result of a mixed-layered structure at these *P-T* conditions composed of both weakly and strongly interacting hydrogen molecules, consistent with the phase predicted computationally (10). Measurements of the infrared spectra demonstrated that hydrogen remains transparent at photon energies down to 0.1 eV at pressures to 360 GPa from a low temperature of 17 K (5) to 340 GPa at 230 K (7), i.e., in the phase fields ascribed to phases III and IV. These results ruled out the claim of a strongly reflecting metal at 270 GPa. These infrared measurements, together with others in the mid-infrared range (higher photon energy) also show that two groups of vibrons exist with distinct *P-T* dependencies, confirming the finding from Raman spectroscopy for two different bonding environments for the hydrogen molecules in phase IV (7–9).

Important information about these transitions has been provided by recent theoretical calculations (10–21). Notably, the type of structure constrained by vibrational spectroscopy for phase IV was among the structures predicted by theory before the experiments (10). These subsequent calculations predict that the structure consists of graphene-structured, honeycomb sheets and molecular interlayers. The molecular layers exhibit higher-frequency vibrons from the stronger molecular bonding, and the graphene sheets are predicted to have less strong bonding, therefore corresponding to the lower-frequency vibron in the vibrational spectra (10, 12–18). As for the question of metallization, the infrared transparency at photon energies down to 0.1 eV (5) rule out a transition to a fully metallic phase; however, phase IV might be a very poor metal, with absorption below 0.1 eV (20, 21), perhaps above a particular range of *P-T* conditions.

Significance

Understanding the behavior of hydrogen under pressure has been a major challenge in modern physics since the early days of quantum mechanics. This paper reports new spectroscopic measurements showing that hydrogen and deuterium transform to complex molecular-based structures to pressures of at least 325 GPa (3.25 megabars). These phases are based on distorted graphene sheets of hydrogen molecules, a major surprise in our understanding of this fundamental system at very high densities. The results provide constraints for theoretical calculations of structures, phase transitions, and electronic properties, including the transition to the predicted metallic state of the solid at 300 K.

Author contributions: C.-s.Z. and R.J.H. designed research; C.-s.Z., R.E.C., and R.J.H. performed research; R.E.C. and R.J.H. contributed new reagents/analytic tools; C.-s.Z., R.E.C., H.-k.M., and R.J.H. analyzed data; and C.-s.Z., R.E.C., H.-k.M., and R.J.H. wrote the paper.

The authors declare no conflict of interest.

[1]To whom correspondence should be addressed. E-mail: rhemley@ciw.edu.

This article contains supporting information online at www.pnas.org/lookup/suppl/doi:10.1073/pnas.1402737111/-/DCSupplemental.

These recent experimental and theoretical efforts have led to new questions about the phase transitions and other physical properties of hydrogen at these multimegabar pressures. The mechanism of the transition to phase IV remains poorly constrained experimentally. There are apparent discrepancies among experiments for the transition pressures and reported evidence for spectral changes that are not understood or are controversial, particularly weak spectral changes near 270 GPa, which tentatively were identified as evidence of a possible new solid phase (6) and the loss of the Raman vibron and the claim of strong metallization (3). Despite the broad agreement between theory and experiment that phase IV has a mixed-layer structure, the detailed structure is not known, and numerous related lower symmetry forms are possible but difficult to predict because of small free energy differences and other challenges of the simulations (9, 13, 14, 16, 17, 19–23). These theoretical studies also predict other phases in the *P-T* range that currently is accessible.

Here we present Raman results that provide information about dense solid hydrogen at multimegabar pressures. In particular, spectroscopic features at 300 K obtained from both isotopes provide evidence for the additional transitions at these conditions. We clarify several outstanding issues and extend measurements to higher pressures for both hydrogen and deuterium. Implications of the transitions for structural and electronic changes (including metallization) and their relation to the transitions at low temperatures are discussed.

Results

Fig. 1 shows the evolution of the Raman spectrum for hydrogen and deuterium to 300 K. There are distinct changes in the high-frequency bands, or vibrons (coupled intramolecular stretches), and their shifts provide important constraints on the state of bonding, intermolecular interactions, and lattice symmetry. Changes in the low-frequency spectra also are observed, and this region contains information related to lattice phonons, librons, and rotons.

The Raman spectrum of vibrons in the region of the I–III–IV transition is shown in Fig. 2. The pressure dependence of the ν_1 vibron for hydrogen changes dramatically at ~216 GPa (213 GPa for D_2); no measurable frequency discontinuity was detected at this pressure. The peak width broadens at this pressure as well. This observation is consistent with previously reported data (3, 4, 7) within reasonable pressure uncertainty. The change is close to the extrapolated I–III boundary; it is important to point out, however, that the pressure dependence of the band is significantly larger than that of phase III, which has been studied extensively at lower temperatures (24, 25). A higher-frequency vibron appears at that pressure as well, and it greatly increases in relative intensity up to ~250 GPa (Fig. 2, *Inset*). This mode was assigned as ν_2 of phase IV (4).

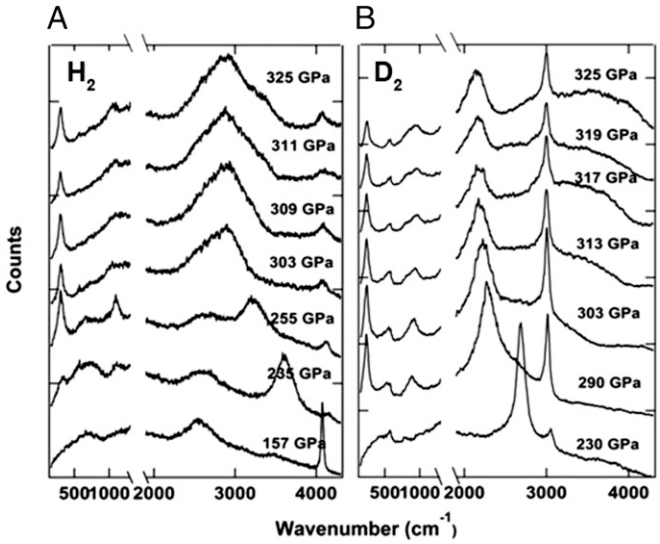

Fig. 1. Selected spectra of hydrogen (*A*) and deuterium (*B*) as a function of pressure at 300 K. The region of the T_{2g} diamond Raman mode has been removed for clarity (*Supporting Information*).

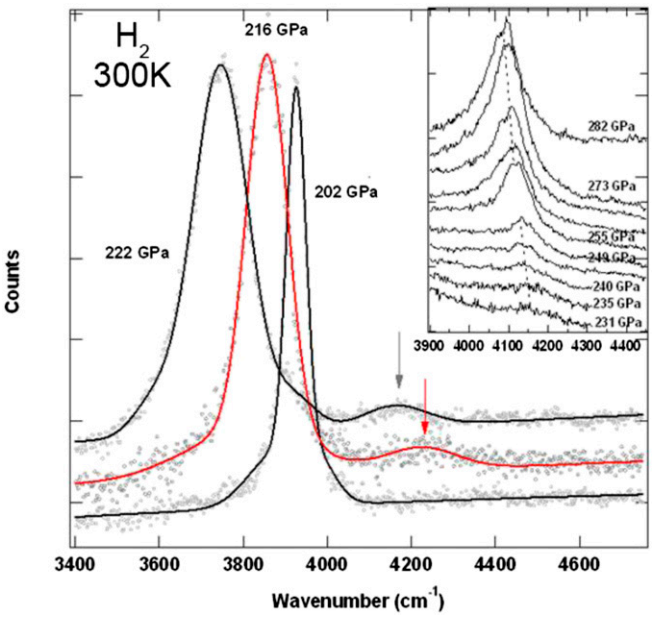

Fig. 2. Hydrogen vibron spectra across the I–III–IV transition. The weak high-frequency vibron (ν_2) appeared at the transition as indicated by the arrows. (*Inset*) Detail in the region of the higher frequency ν_2 peak to higher pressures (see *Supporting Information*).

Fig. 3 shows details of the Raman spectrum from selected runs above 300 GPa for the two isotopes. At these higher pressures, additional features (shoulders) develop, or the lineshape appears to change for the stronger lower-frequency vibron band ν_1 for both isotopes. The overall band may be fitted with two components (*Supporting Information*). Fig. 3 also shows a detail of selected low-frequency Raman spectra. The most striking feature is an abrupt intensity decrease for the lowest-frequency mode and a new peak appearing near ~1,000 cm^{-1} at almost the same pressure (~285 GPa) for hydrogen (*Supporting Information*). Above this pressure, the intensity of the lowest-frequency mode changes and persists to the highest pressure of this study, whereas the new peak splits further at ~300 GPa. On the other hand, no intensity change was observed in the lowest-frequency band in deuterium at 285 GPa.

The pressure dependence of the vibron frequencies for hydrogen and deuterium at 300 K from multiple experimental runs are plotted in Fig. 4, along with previously reported results over a range of pressures (8, 9, 26). There is broad agreement with trends in the pressure shifts reported previously for the pressure dependence of the frequencies, although there also are some significant differences. The pressure dependence for ν_1 band shows a slight slope change at 285 GPa, becoming almost flat after 300 GPa. Above 300 GPa and 310 GPa for hydrogen and deuterium, respectively, a weak feature appears on the high-frequency side of the ν_1 vibron (see *Supporting Information*). With increasing pressure, the frequency of this feature steeply increases, whereas the pressure slope of ν_1 frequency is reduced further. Detailed inspection also reveals the evidence for weak changes in the slope of

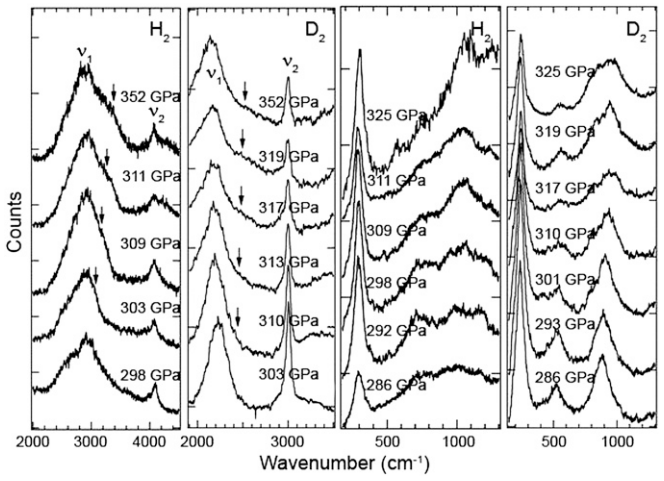

Fig. 3. Detail of Raman spectra of hydrogen and deuterium at the highest pressures from selected runs.

ν_2 near 285 GPa and 300 GPa in both isotopes (and near 250 GPa in hydrogen).

The pressure dependence of the low-frequency bands is shown in Fig. 5. The low-frequency spectra change near 250 and 285 GPa in both hydrogen and deuterium. In particular, there is evidence for a change in the pressure dependence of the highest-frequency phonons near 285 GPa. The low-frequency peaks appearing at 285 GPa (~1,000 cm^{-1} for hydrogen and ~850 cm^{-1} for deuterium) split at 300 GPa and 310 GPa for H_2 and D_2, respectively. In deuterium, a new peak appears at ~850 cm^{-1} and splits at 310 GPa. On the other hand, as noted above, no intensity change was observed in the lowest-frequency band in deuterium.

Discussion

I–III–IV Transition. Previously reported experiments (3–9) all imply the same I–III–IV phase sequence at 300 K, although different transition pressures and transition criteria are reported. Eremets and Troyan (3) originally reported three Raman modes for hydrogen above 220 GPa at room temperature, including a low-frequency peak at 304 cm^{-1} and a high-frequency vibron at ~4,150 cm^{-1}. They attributed the appearance of these bands to a transition to the metallic *Cmca*-12 phase. The same peaks were found by Howie et al. (4) at 235 GPa and used to assign the transition to phase IV. The lowest-frequency mode becomes prominent in our spectra near 225 GPa and with a further increase in pressure, exhibits a steady intensity increase and a slight decrease in frequency for both isotopes (Fig. 5). Theoretical calculations (15) indicate that this peak is a librational mode in the graphene-like layer of the proposed structures.

The most prominent feature associated with the transition at these temperatures is behavior of the strong Raman vibron (ν_1) (3, 4). Early Raman measurements were carried out above 200 GPa at 300 K, but scatter in the data precluded identification of a transition (27). Loubeyre et al. (9) reported a very small discontinuity in the pressure dependence of the ν_1 vibron frequency at 215 GPa. However, a large change in the pressure dependence of the frequency similar to that reported by others was found at 237 GPa. In addition, the high-frequency vibron mode (ν_2) attributed to phase IV (4) also appeared at this pressure. The ν_2 mode has been assigned to the vibron stretch molecules in a new layer not present in the structure of phase III (10, 13, 14, 17). Loubeyre et al. (9) questioned the previously assigned stability region of phase III at 300 K, but the pressure offset of the results of that study compared with the others suggests an overestimation of the pressure. A correction of 20 GPa, for example, would bring the transition they reported at 237 GPa to 217 GPa, in agreement with our data and reasonably consistent with the other work. We emphasize that these pressures are all relative to the diamond Raman scale used in these studies.

We considered the possibility that the transition might be to a new phase near 216 GPa (e.g., III′). We note that the effect of pressure on the temperature derivative of the ν_1 frequency becomes negative at this pressure (Fig. 4: compare 100 K and 300 K data). There is evidence for a discontinuity in frequency of the principal Raman vibron across the III–IV transition. This discontinuity is *P-T* dependent, decreasing significantly with increasing temperature (6). The phase thus is characterized by a very steep pressure dependence of the ν_1 vibron frequency, almost four times that of the established lower-temperature phase III. If a high-temperature phase III′ exists, it must be closer in

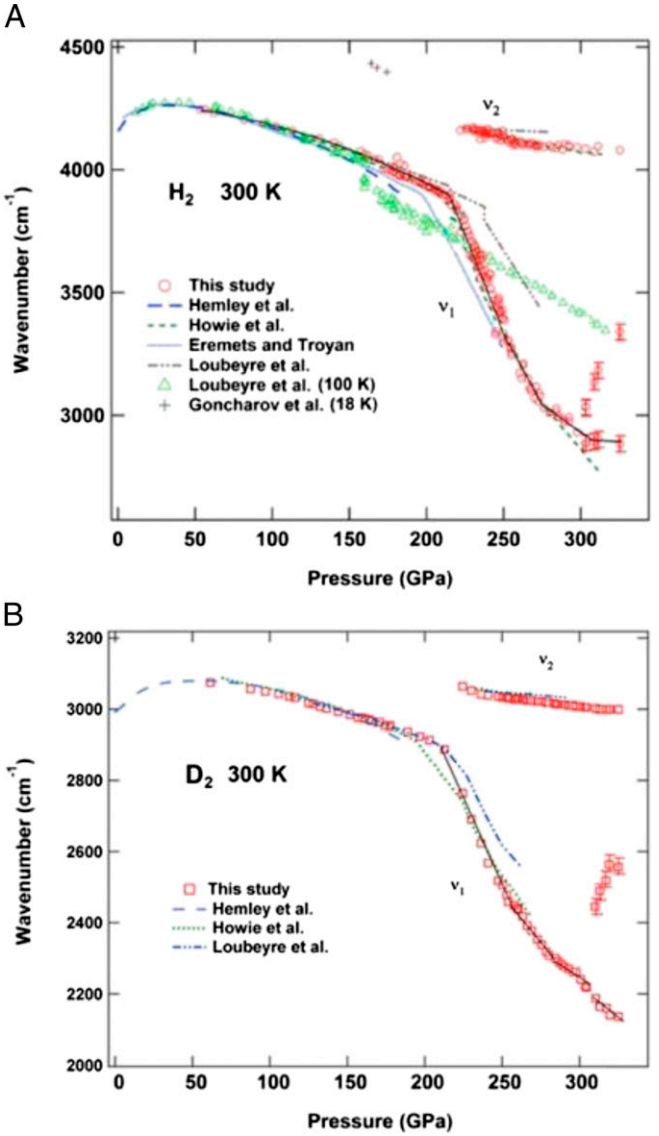

Fig. 4. Pressure dependence of Raman vibrons at 300 K. (*A*) Hydrogen. Previous 300-K results from Howie et al. (4), Eremets and Troyan (3), and Loubeyre et al. (9), as well as the low-temperature data from Loubeyre et al. (37) and Goncharov et al. (28), are shown. (*B*) Deuterium. Previous results from Hemley et al. (26, 38), Howie et al. (4), and Loubeyre et al. (9) are shown. Spectral changes are evident at the indicated pressures. The error bars for the data points above 300 GPa are estimated from the peak fit to the background-subtracted spectra (*Supporting Information*).

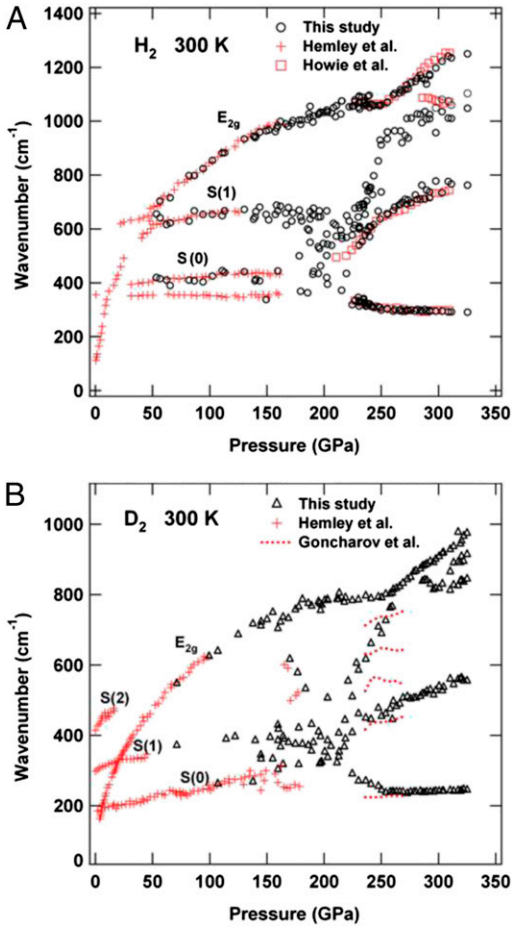

Fig. 5. Pressure dependences of the lower frequency for hydrogen Raman frequencies (*A*) and deuterium (*B*). Previous results from Hemley et al. (38, 39), Howie et al. (4), and Goncharov et al. (15) are shown.

structure to phase III than phase IV, which is consistent with detailed IR measurements at these conditions (7).

The feature identified as ν_2 appears indicative of phase IV (e.g., at 216 GPa). A question arises as to whether the very weak high-frequency peak observed in phase III at 18 K and lower pressures (28) is related to the phase IV ν_2 vibron. If so, this would suggest a possible relationship between the two phases. However, the frequencies and intensities of the two bands are distinct, and the features are observed in different *P-T* regions. For example, vibron–libron combination Raman bands in phase III must be ruled out. Nevertheless, a possible connection between the two phases should be explored with additional measurements that would allow tracking of the behavior of the higher-frequency feature documented in phase III up to the transition to phase IV.

The above analysis leads to the proposition that the phase III pressure interval at 300 K is narrow (~10 GPa), consistent with the proximity to the proposed I–III–IV triple point (7). This would indicate that the phase I–III transition at 300 K is close to 200–205 GPa (again, on the diamond Raman pressure scale). We point out that the III–IV transition is observed more clearly in IR than Raman measurements (7). By comparison, the I–III boundary is less well defined by both spectroscopies at these temperatures. The results have implications for the mechanism of the transition sequence from phase I to IV in this *P-T* range. The III–IV transition may occur with the initial formation of a few layers of weakly interacting molecules followed by the creation of ordered alternating layers before ultimately forming a more well-defined structure (10). The thermodynamically stable phases must be ordered, but they might have a longer repeat unit. In fact, recent theoretical calculations predict stability of a doubled repeat unit having two types of distorted graphene-structured layers (18). Even longer sequences are possible, but given the low driving force near the transition, the molecular sheets may occur initially as stacking faults.

Spectral Changes at 250, 285, and 300 GPa. Weaker spectral changes are observed at higher pressure on room temperature compression. We first consider the behavior near 250 GPa. There might be a change in pressure dependence of ν_1 near that pressure (Fig. 4), although the scatter and variations in frequencies from run to run preclude identification of a definite change, which is consistent with the scatter reported in previous studies (e.g., ref. 29). Moreover, there is no evidence within experimental error for changes in ν_1 for deuterium at that pressure (Fig. 4). However, the pressure dependence of the lowest-frequency mode in that isotope changes near 250 GPa, and there are variations in frequencies of other low-frequency bands in that region (Fig. 5). Also, the intensity of a higher-frequency phonon mode at ~1,050 cm^{-1} at 250 GPa changes abruptly (*Supporting Information*), which is consistent with that reported by Eremets and Troyan (3). There also is evidence for weak changes in pressure dependence of the frequency, linewidth, and intensity of ν_2 near 250 GPa (Figs. 2 and 4 and *Supporting Information*).

Multiple runs show the same abrupt intensity decrease of the lowest-frequency peak (initially at 308 cm^{-1} in hydrogen), and the new peak appearing around 1,000 cm^{-1} at similar pressures of ~285 GPa; above this pressure, the intensity of the lowest-frequency mode changes but persists to the highest pressures, whereas the new peak splits at ~300 GPa. The change in the low-frequency spectra near 285 GPa for hydrogen also occurs in deuterium starting at the same pressure, with a new peak appearing at ~850 cm^{-1} and splitting at 310 GPa. On the other hand, no intensity changes were observed in the lowest-frequency band in deuterium at 285 GPa.

The changes in low-frequency modes, as well as in the pressure dependence of ν_1 vibron frequency at 285 GPa, imply possible structural changes at this pressure. A small change in slope of the ν_1 vibron frequency was reported previously at 275 GPa (6), which the authors suggested as the indication of a transition to a structurally related phase, which they called phase IV′. Because the spectral changes are not dramatic, this change is distinct from the claim in ref. 3 for a loss of Raman vibron spectrum and the transition to a dark and electrically conducting phase around that pressure. Peaks from the Raman vibrons and lower frequency excitations persist through this pressure interval, although we found evidence for an overall weakening of the spectrum in the lower-frequency region at these pressures (*Supporting Information*).

Peak splitting in both principal vibron and low-frequency modes above 300 GPa at 300 K indicates a possible transition at these conditions. These spectral changes were not reported previously (4). The changes in both principal vibrons and lattice modes for both isotopes indicate a new transition. Hydrogen and deuterium exhibit similar changes on compression with respect to possible discontinuities in the pressure dependence of vibrons and lattice modes, although some of the pressures do not coincide. We suggest that the differences might be the result of uncertainties in the pressure determination. The differences in spectroscopic behavior of these two isotopes at these pressures are discussed in detail elsewhere.

Complex Sequence of Transitions. The above analysis indicates that several transitions may occur on compression of hydrogen and deuterium at 300 K in the region previously identified as the

stability field of phase IV. The overall similarities in the spectra indicate variations in the structure of phase IV. As such, these may be identified tentatively as phases IV″ (250 GPa), IV′ (~285 GPa), and IV‴ (300 GPa). Alternatively, these might be truly distinct phases (V, VI, VII, etc.), although they may not correspond to structures predicted theoretically and identified with these labels. As described above, vibrational spectroscopic data, together with density functional theory (DFT) computations, suggest that phase IV is a mixed-layer structure, with honeycomb or graphene-structured sheets separated by molecular H_2 layers (14). First-principles classical molecular dynamics indicates that the molecules in the H_2 layers are quantum rotators (17), and even the graphene layers may be dynamic (18). As discussed below, the structures may differ according to changes in rotational ordering, weak structural distortions, and/or changes in electronic structure (e.g., degree of band overlap). Indeed, we point out that there may not be a unique, classical structure in view of potentially large quantum fluctuations or fluxional behavior of hydrogen at these conditions. Nevertheless, it is useful to examine these possibilities in terms of the expected Raman modes assuming classical proposed structures.

An idealized, phase IV structure having space group symmetry *Pbcn* has been proposed for the phase (14). Distortions of structure derived from this structure and having space groups P_c and C_c have been proposed (14, 17). There are 48 Raman-active modes for the *Pbcn* structure, $12A_g$, $12B_{1g}$, $12B_{2g}$, and $12B_{3g}$ modes, but it is likely that only the A_g modes have significant intensity, and the majority of these modes may be weak and give rise to broadened or barely observable peaks. In *Pbcn*, the interlayer molecules fill two symmetrically distinct sites, so there would be two vibrons, perhaps a closely spaced doublet. If one considers the same structure but with rotating H_2 molecules in the interlayer, one rotating molecule sits at the Wyckoff position 4a and contributes no Raman modes other than its vibron; the other contributes four Raman modes from the molecular motions, each with a different symmetry (A_g, B_{1g}, B_{2g}, and B_{3g}), which would increase the number of modes by two relative to the ordered *Pbcn* structure without rotating molecules. However, a small distortion of this structure brings it to the highly symmetric *P6/mmm* structure, with graphene layers of hydrogen alternating with rotating layers that are hexagonal nets. There are then only two Raman-active modes: a single vibron in the molecular layers and a doubly degenerate E_{2g} mode to the graphene layers. Because the distortion of this structure is small, we expect to see only two intense Raman modes, consistent with ν_1 for the sheets and ν_2 for the molecular layers.

Fig. 6 compares the Raman vibron shifts with pressure for the two isotopes, as well as the results of recent theoretical calculations for phase IV. The calculations are for the P_c structure, which is similar to *Pbcn* but with slight distortions of the graphene-like layers. The calculated vibron frequencies for P_c from 250 GPa to 370 GPa (15) are in qualitative agreement with experiment. For example, the weak pressure dependence of the calculated ν_2 frequency from 300 GPa to 370 GPa is consistent with the present results. There is a large mismatch in some frequencies (e.g., for ν_1). The latter likely arises from strong quantum anharmonicity that is not included in the calculations and the fluxional character of the system as noted above, but it also might be the result of detailed differences in structure between theory and experiment.

There are several candidates for the higher-pressure transitions. DFT calculations predict stability of the *Cmca*-4 structure at these conditions (13, 17, 30, 31). Interestingly, the *Cmca*-4 structure is predicted to have a very high superconducting T_c (32). The phonons in the *Cmca*-4 structure are predicted to be significantly softer than those in phase IV (14), which appears inconsistent with experiment. Another transition would be freezing of the molecular rotations in phase IV, leading to a structure with

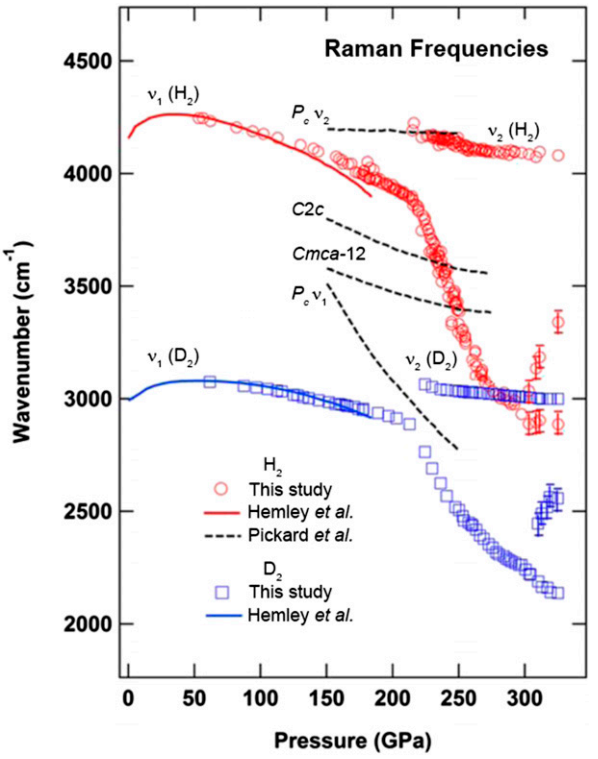

Fig. 6. Comparison of experimental and theoretical Raman vibron frequencies for dense hydrogen and deuterium. Experimental results at 300 K (26) and theoretical calculations for the static lattice of candidate structures (14) are shown.

puckered honeycomb sheets. It does not seem that this would cause splitting of ν_1 in the sheets, so this is not a good candidate for the changes occurring near 300 GPa but may be associated with the 285-GPa transition. If so, the higher-pressure changes might be associated with the transition to *Cmca*-12 (10, 14). Hybrid and van der Waals functional static lattice calculations show *Cmca*-12 to be more stable than *Cmca*-4 (16). A third possibility is metallization or even a metal-to-insulator transition with increasing pressure, as observed for the heavier alkalis Na (33, 34) and Li (35).

As discussed above, theoretical calculations indicate that phase IV can be conductive at the conditions studied here. However, the predicted structures have only a small density of states at the Fermi level (20, 21). No infrared absorption that is clearly diagnostic of a metallic state has been observed at the *P-T* conditions explored so far for the solid (7). The increase in phonon linewidths at 285 GPa is consistent with the onset of metallicity with the broadening caused by electron–phonon scattering. It is possible that phase IV is metallic even when it forms, as predicted by DFT, but the density of states may be too small initially to affect phonon linewidths significantly, because metallization occurs only at isolated pockets in the Brillouin zone, or correlations and/or quantum and thermal disorder may lead to localization and insulating behavior. Thus, the apparent transition near 285 GPa may be associated with changes in, or enhancement of, band overlap. If so, the transition might be accompanied by an increase in electrical conductivity, although we emphasize that hydrogen remains molecular and transparent in the visible and near IR at these pressures and temperatures (300 K). We suggest that spectral changes observed near 300 GPa may arise from partial freezing of the rotations of the H_2 molecules. It also is possible that this occurs together with some reconstruction to a phase having a different classical space group (e.g., *Cmca*-12).

Conclusions

Raman measurements provide information on the nature of transitions to dense solid phases of hydrogen and deuterium to 325 GPa at 300 K. The transition to phase III at 300 K may occur with the nucleation of a few layers of weakly interacting molecules, with the creation of ordered alternating layers occurring over a range of pressures, and the transitions may be higher order. We observe changes in hydrogen at 300 K at pressures of 250, 285, and 300 GPa. The changes at 285 GPa suggest the possible onset of metallicity that broadens the phonon linewidths by electron–phonon scattering. The transition at 300 GPa may represent a structural transition (e.g., phase V). The results indicate the existence of changes in structure and bonding, molecular orientational order, and electronic structure of dense hydrogen. Hydrogen could parallel the behavior of Li and Na, which crystallize in complex phases and transitions near their high-pressure melting minima. The behavior of hydrogen at these conditions thus is more complex than expected and predicted by theory. Continued experiments at higher pressures over a broad range of temperature are needed to provide information on this fundamental system under extreme conditions.

Methods

Ultrahigh-purity normal hydrogen gas was loaded into tungsten gaskets of diamond anvil cells at ~0.2 GPa; then, the pressure was raised to tens of gigapascals soon after the loading. The sample sizes typically ranged between 2 μm and 6 μm when the pressure was above 300 GPa. Backscattering geometry was used, with both 532-nm and 633-nm laser lines as the Raman excitation wavelength. Experimental data for a total of six runs are reported here. Samples were compressed and measurements were conducted at room temperature. Because of the limitations of sample volume, no ruby or other pressure sensors were loaded into the sample chamber. Pressure was determined from the sharp edge of the first-order diamond Raman band produced at the diamond–sample surface of the stressed anvil. A shift of 1,860 cm^{-1} of the peak, for example, corresponds to 325 GPa on the diamond pressure scale (36). Approximately 30 runs to multimegabar pressures were carried out over a 3-y period (see *Supporting Information* for additional experimental details).

ACKNOWLEDGMENTS. We are grateful to R. Boehler, M. Ahart, Z. Liu, V. V. Struzhkin, T. Strobel, M. Somayazulu, A. F. Goncharov, D. Klug, R. Hoffmann, and S. A. Gramsch for valuable discussions and assistance and to the reviewers for very helpful recommendations that improved the paper. This research was supported by the National Science Foundation (DMR-1106132), the Department of Energy (DOE)/National Nuclear Security Administration (DE-NA000006; Carnegie/Department of Energy Alliance Center, CDAC), and the DOE Office of Science/Basic Energy Sciences (DE-SC0001057; EFree, an Energy Frontier Research Center).

1. Mao HK, Hemley RJ (1994) Ultrahigh-pressure transitions in solid hydrogen. *Rev Mod Phys* 66(2):671–692.
2. McMahon JM, Morales MA, Pierleoni C, Ceperley DM (2012) The properties of hydrogen and helium under extreme conditions. *Rev Mod Phys* 84(4):1607–1653.
3. Eremets MI, Troyan IA (2011) Conductive dense hydrogen. *Nat Mater* 10(12):927–931.
4. Howie RT, Guillaume CL, Scheler T, Goncharov AF, Gregoryanz E (2012) Mixed molecular and atomic phase of dense hydrogen. *Phys Rev Lett* 108(12):125501.
5. Zha CS, Liu Z, Hemley RJ (2012) Synchrotron infrared measurements of dense hydrogen to 360 GPa. *Phys Rev Lett* 108(14):146402.
6. Howie RT, Scheler T, Guillaume CL, Gregoryanz E (2012) Proton tunneling in phase IV of hydrogen and deuterium. *Phys Rev B* 86(21):214104.
7. Zha CS, Liu Z, Ahart M, Boehler R, Hemley RJ (2013) High-pressure measurements of hydrogen phase IV using synchrotron infrared spectroscopy. *Phys Rev Lett* 110(21): 217402.
8. Eremets MI, Troyan IA, Lerch P, Drozdov A (2013) Infrared study of hydrogen up to 310 GPa at room temperature. *High Press Res* 33(2):377–380.
9. Loubeyre P, Occelli F, Dumas P (2013) Hydrogen phase IV revisited via synchrotron infrared measurements in H_2 and D_2 up to 290 GPa at 296 K. *Phys Rev B* 87(13): 134101.
10. Pickard CJ, Needs RJ (2007) Structure of phase III of solid hydrogen. *Nat Phys* 3(7): 473–476.
11. Labet V, Gonzalez-Morelos P, Hoffmann R, Ashcroft NW (2012) A fresh look at dense hydrogen under pressure. I. An introduction to the problem, and an index probing equalization of H-H distances. *J Chem Phys* 136(7):074501.
12. Lebègue S, et al. (2012) Semimetallic dense hydrogen above 260 GPa. *Proc Natl Acad Sci USA* 109(25):9766–9769.
13. Liu H, Zhu L, Cui W, Ma Y (2012) Room-temperature structures of solid hydrogen at high pressures. *J Chem Phys* 137(7):074501.
14. Pickard CJ, Martinez-Canales M, Needs RJ (2012) Density functional theory study of phase IV of solid hydrogen. *Phys. Rev. B* 85(21):214114; (2002) Erratum: Density functional theory study of phase IV of solid hydrogen. *Phys Rev B* 86(5):059902.
15. Goncharov AF, et al. (2013) Bonding, structures, and band gap closure of hydrogen at high pressures. *Phys Rev B* 87(2):024101.
16. Li XZ, et al. (2013) Classical and quantum ordering of protons in cold solid hydrogen under megabar pressures. *J Phys Condens Matter* 25(8):085402.
17. Liu H, Ma Y (2013) Proton or deuteron transfer in phase IV of solid hydrogen and deuterium. *Phys Rev Lett* 110(2):025903.
18. Magdau IB, Ackland GJ (2013) Identification of high-pressure phases III and IV in hydrogen: Simulating Raman spectra using molecular dynamics. *Phys Rev B* 87(17): 174110.
19. Morales MA, McMahon JM, Pierleoni C, Ceperley DM (2013) Towards a predictive first-principles description of solid molecular hydrogen with density functional theory. *Phys Rev B* 87(18):184107.
20. Naumov II, Cohen RE, Hemley RJ (2013) Graphene physics and insulator-metal transition in compressed hydrogen. *Phys Rev B* 88(4):045125.
21. Cohen RE, Naumov II, Hemley RJ (2013) Electronic excitations and metallization of dense solid hydrogen. *Proc Natl Acad Sci USA* 110(34):13757–13762.
22. Magdau IB, Ackland GJ (2013) High temperature Ranam analysis of hydrogen phase IV from molecular dynamics. arXiv:1307.7378v1 [cond-mat.mtrl-sci].
23. Liu H, Tse JS, Ma Y (2013) Robust diffusive proton motions in phase IV of solid hydrogen. arXiv:1311.7086v2 [cond-mat.mtrl-sci].
24. Goncharov AF, Mazin II, Eggert JH, Hemley RJ, Mao Hk (1995) Invariant points and phase transitions in deuterium at megabar pressures. *Phys Rev Lett* 75(13):2514–2517.
25. Mazin II, Hemley RJ, Goncharov AF, Hanfland M, Mao HK (1997) Quantum and classical orientational ordering in solid hydrogen. *Phys Rev Lett* 78(6):1066–1069.
26. Hemley RJ, Mao HK, Hanfland M (1991) Spectroscopic investigations of the insulator-metal transition in solid hydrogen. *Molecular Systems Under High Pressure*, eds Pucci R, Piccitto G (Elsevier, Amsterdam), pp 223–243.
27. Ruoff AL (1996) *High Pressure Science and Technology*, ed Trzecialkowski WA (World Scientific, Singapore), pp 511–516.
28. Goncharov AF, Hemley RJ, Mao HK, Shu J (1998) New high-pressure excitations in parahydrogen. *Phys Rev Lett* 80(1):101–104.
29. Howie RT, Gregoryanz E, Goncharov AF (2013) Hydrogen (deuterium) vibron frequency as a pressure comparison gauge at multi-Mbar pressures. *J Appl Phys* 114(7): 073505.
30. Ashcroft NW (1991) Optical response near a band overlap: Application to dense hydrogen. *Molecular Systems Under High Pressure*, eds Pucci R, Piccitto G (Elsevier, Amsterdam), pp 201–222.
31. Edwards B, Ashcroft NW, Lenosky T (1996) Layering transitions and the structure of dense hydrogen. *Europhys Lett* 34(7):519–524.
32. Cudazzo P, et al. (2008) Ab initio description of high-temperature superconductivity in dense molecular hydrogen. *Phys Rev Lett* 100(25):257001.
33. Lazicki A, et al. (2009) Anomalous optical and electronic properties of dense sodium. *Proc Natl Acad Sci USA* 106(16):6525–6528.
34. Ma Y, et al. (2009) Transparent dense sodium. *Nature* 458(7235):182–185.
35. Matsuoka T, Shimizu K (2009) Direct observation of a pressure-induced metal-to-semiconductor transition in lithium. *Nature* 458(7235):186–189.
36. Akahama Y, Kawamura H (2004) High-pressure Raman spectroscopy of diamond anvils to 250 GPa: Method for pressure determination in the multimegabar pressure range. *J Appl Phys* 96(7):3748–3751.
37. Loubeyre P, Occelli F, LeToullec R (2002) Optical studies of solid hydrogen to 320 GPa and evidence for black hydrogen. *Nature* 416(6881):613–617.
38. Hemley RJ, Eggert JH, Mao HK (1993) Low-frequency Raman spectroscopy of deuterium to megabar pressure at 77-295 K. *Phys Rev B* 48(9):5779–5788.
39. Hemley RJ, Mao HK, Shu JF (1990) Low-frequency vibrational dynamics and structure of hydrogen at megabar pressures. *Phys Rev Lett* 65(21):2670–2673.

Supporting Information

Zha et al. 10.1073/pnas.1402737111

SI Text

Samples were prepared using techniques similar to those described in refs. 1 and 2. Fig. S1 shows representative diamond-edge spectra used for pressure calibration (3–6). The zone-center optical phonon Raman mode of diamond is triply degenerate and remains a singlet under isotropic (hydrostatic) stress. Uniaxial stress of the anvils in these geometries splits the T_{2g} peak into a doublet or triplet on the high-energy edge. These peaks have different pressure (stress) dependences and have not been calibrated at the high pressures of these experiments (7). The intensity of this sharp peak is proportional to the size of the sampled area in our experiments, and nonhydrostatic stresses produce a steep edge in the high-energy end of the spectrum with no peak. The anvil geometry and shape also affect the pressure shift of the Raman peak (8). All experiments reported here used the anvils with [100] crystal axis in the force-loading direction and tip dimension parameters similar to those reported by others. Nevertheless, the pressure calibration discrepancy between this study and others cannot be avoided. Measurements of the vibron frequency provide a consistency check among different studies (9).

Additional spectra are shown in the remaining figures. Fig. S2 shows the pressure dependence of vibron linewidth for hydrogen. Linewidth of ν_1 changed gradually with pressure, with an abrupt increase at 216 GPa. A significant broadening after 285 GPa also can be seen. Low-frequency Raman spectra are shown in Fig. S3. Changes in phonon spectra at 250 GPa can be seen in the second panel from the left. Around 285 GPa, both runs show similar spectral changes. The lower intensity at this pressure appears to recover and persists to the highest pressure, and a peak appears at ∼1,000 cm^{-1} and further splits after ∼300 GPa (Fig. 5). The results of the fits of the vibron spectra for H_2 and D_2 at the highest pressures are shown in Figs. S4 and S5.

1. Zha CS, Liu Z, Hemley RJ (2012) Synchrotron infrared measurements of dense hydrogen to 360 GPa. *Phys Rev Lett* 108(14):146402.
2. Zha CS, Liu Z, Ahart M, Boehler R, Hemley RJ (2013) High-pressure measurements of hydrogen phase IV using synchrotron infrared spectroscopy. *Phys Rev Lett* 110(21): 217402.
3. Akahama Y, Kawamura H (2004) High-pressure Raman spectroscopy of diamond anvils to 250GPa: Method for pressure determination in the multimegabar pressure range. *J Appl Phys* 96:3748.
4. Akahama Y, Kawamura H (2005) Raman study on the stress state of [111] diamond anvils at multimegabar pressure. *J Appl Phys* 98:083523.
5. Akahama Y, Kawamura H (2006) Pressure calibration of diamond anvil Raman gauge to 310GPa. *J Appl Phys* 100:043516.
6. Loubeyre P, Occelli F, LeToullec R (2002) Optical studies of solid hydrogen to 320 GPa and evidence for black hydrogen. *Nature* 416(6881):613–617.
7. Grimsditch MH, Anastassakis E, Cardona M (1978) Effect of uniaxial stress on the zone-center optical phonon of diamond. *Phys Rev B* 18(2):901–904.
8. Baer BJ, Chang ME, Evans WJ (2008) Raman shift of stressed diamond anvils: Pressure calibration and culet geometry dependence. *J Appl Phys* 104:034504.
9. Howie RT, Gregoryanz E, Goncharov AF (2013) Hydrogen (deuterium) vibron frequency as a pressure comparison gauge at multi-Mbar pressures. *J Appl Phys* 114:073505.

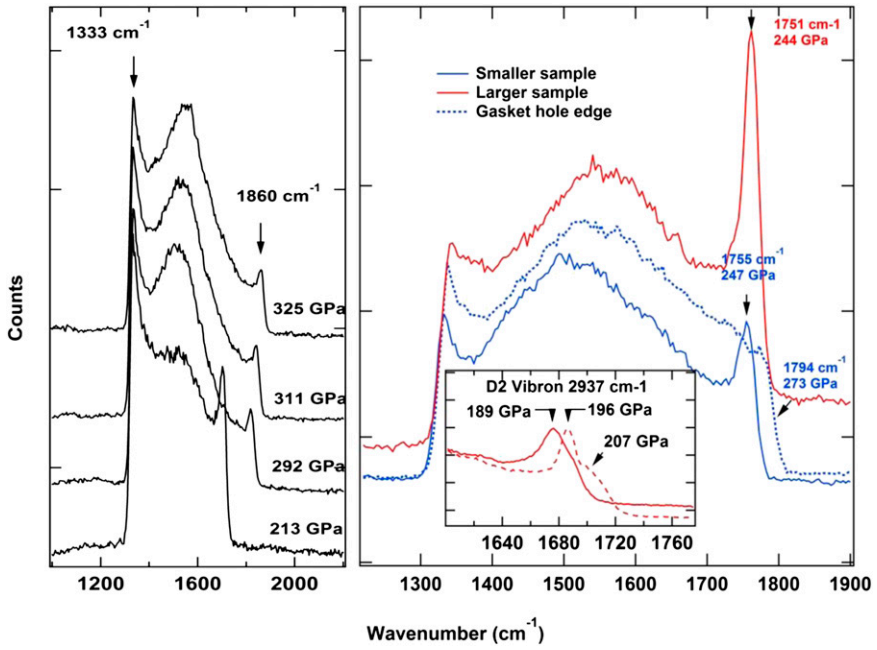

Fig. S1. (*Left*) First-order diamond Raman spectra at different pressures. (*Right*) The intensity of the sharp peak at the high-frequency end of the spectra is proportional to the sample size; the red and blue solid line spectra were collected from samples with diameters of ~5 μm and ~15 μm, respectively. The blue dotted line spectrum was collected from the gasket portion near the hole edge, and no sharp high- frequency peak is observed because of inhomogeneous, nonhydrostatic stresses. (*Inset*) The red solid line spectrum is collected from the anvil with [100] crystal axis in the loading direction; the red dashed line spectrum was measured from an anvil with arbitrary (unknown) crystal orientation in the force-loading direction.

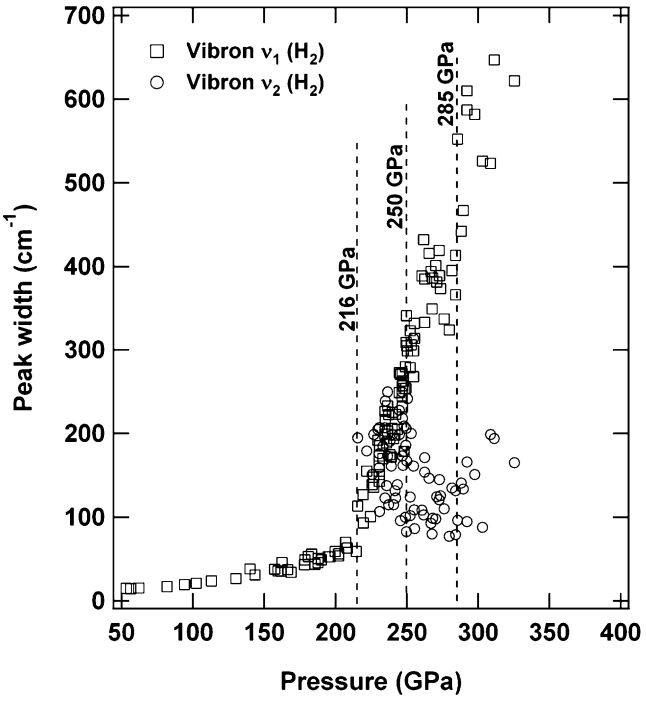

Fig. S2. Pressure dependence of the linewidth of the vibrons for hydrogen, showing changes near 216, 250, and 285 GPa.

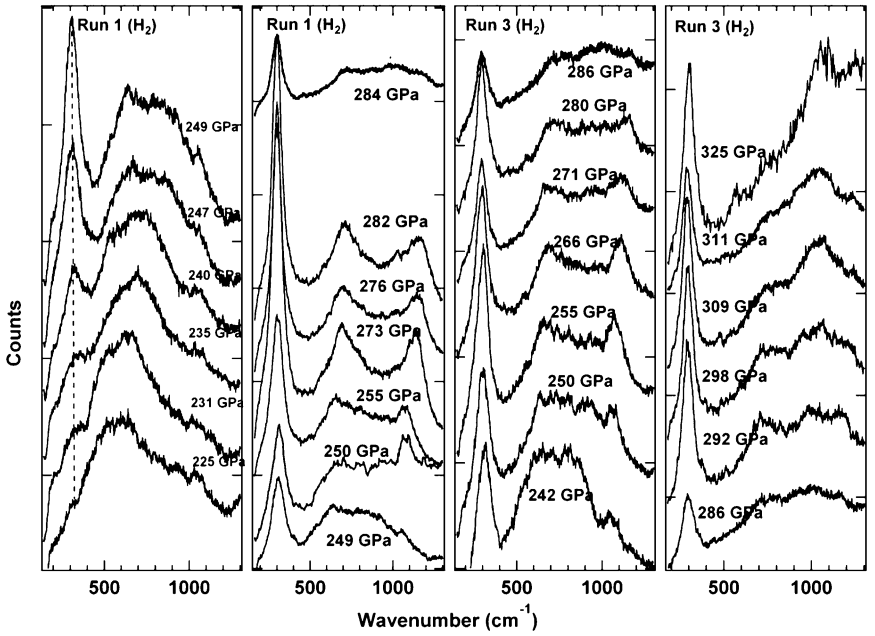

Fig. S3. Selected low-frequency spectra of hydrogen as a function of pressure from two different runs.

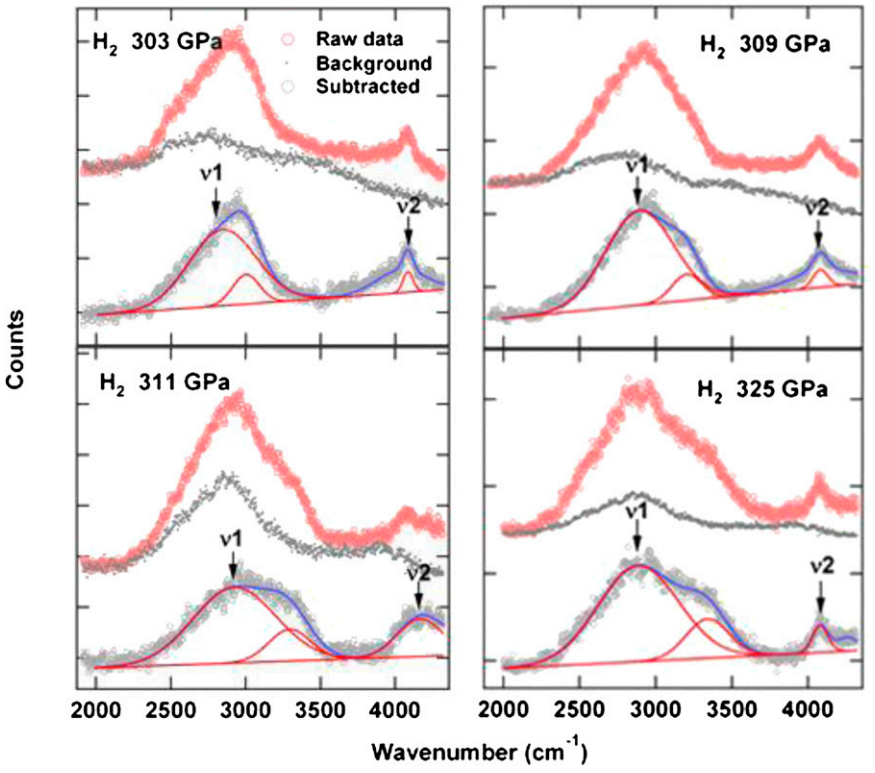

Fig. S4. Fitting results in the high-frequency vibron region of hydrogen.

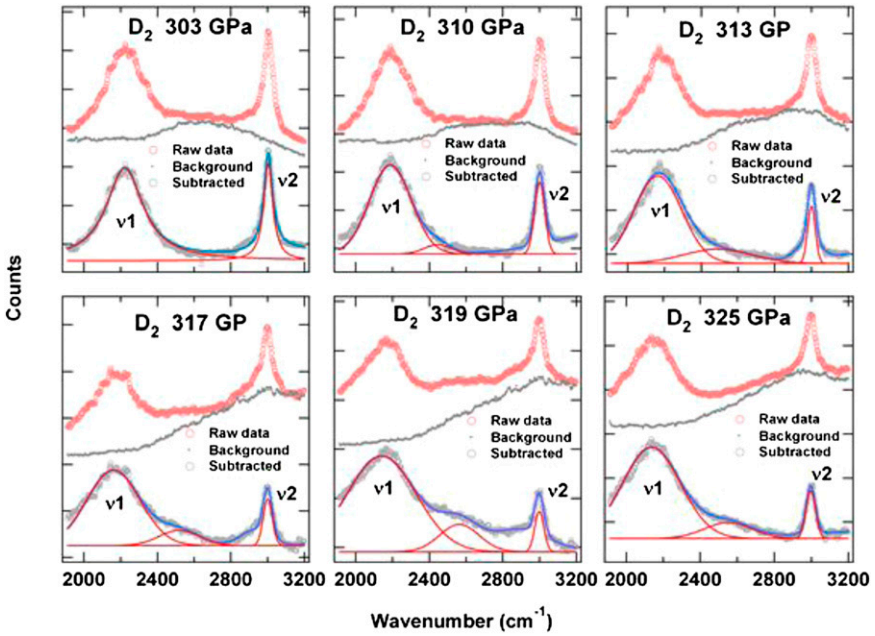

Fig. S5. Fitting results in the high-frequency vibron region of deuterium.